Journal of Pharmaceutical Research International

33(39B): 308-319, 2021; Article no.JPRI.72038
ISSN: 2456-9119
(Past name: British Journal of Pharmaceutical Research, Past ISSN: 2231-2919, NLM ID: 101631759)

Computational Screening of FDA Approved Drugs from ZINC Database for Potential Inhibitors of Zika Virus NS2B/NS3 Protease: A Molecular Docking and Dynamics Simulation Study

Hasanain Abdulhameed Odhar[1*], Salam Waheed Ahjel[1] and Zanan Abdulhameed Odhar[2]

[1]Department of pharmacy, Al-Zahrawi University College, Karbala, Iraq.
[2]Ministry of Health, Baghdad, Iraq.

Authors' contributions

This work was carried out in collaboration among all authors. All authors read and approved the final manuscript.

Article Information

DOI: 10.9734/JPRI/2021/v33i39B32208
Editor(s):
(1) Dr. Syed A. A. Rizvi, Nova Southeastern University, USA.
Reviewers:
(1) Kalpana, Dr. Ambedkar Institute of Technology, India.
(2) Anna Luganini, University of Turin, Italy.
Complete Peer review History: https://www.sdiarticle4.com/review-history/72038

Original Research Article

Received 25 May 2021
Accepted 29 July 2021
Published 03 August 2021

ABSTRACT

Zika virus is a mosquito borne pathogen with a single strand RNA genome. Human infection with this virus is usually asymptomatic, however outbreaks reported in both Pacific region and Latin America have been associated with increase in frequency of microcephaly in newborns and fetuses of infected mothers. Also, the incidence of Guillain-Barré syndrome had also increased among adults with Zika virus infection. Currently, neither vaccine nor antiviral drug has been developed against Zika virus. Structure based virtual screening can be employed, through drug repurposing strategy, to accelerate the identification of potential anti-Zika virus candidates. As such, virtual screening of approved drugs against Zika virus NS2B/NS3 protease can help to recognize new hits capable of hindering viral ability to replicate and evade immune system of the host. In this computational study, we have screened 1615 FDA approved drugs against NS2B/NS3 protease enzyme of Zika virus by using both molecular docking and dynamics simulation. Our virtual screening results indicate that the anti-muscarinic agent Darifenacin and the anti-diarrheal agent

**Corresponding author: E-mail: hodhar3@gmail.com;*

Loperamide may have a promising capacity to inhibit Zika virus NS2B/NS3 protease. According to molecular docking and dynamics simulation, these two approved drugs have good binding capacity to NS2B/NS3 as reported by docking energy of binding and MM-PBSA binding energy. In addition, both Darifenacin and Loperamide were able to maintain close proximity to protease crystal throughout simulation period. However, invitro evaluation of these two drugs against Zika virus NS2B/NS3 protease is required to confirm these computational results.

Keywords: Zika virus; NS2B/NS3 protease; structure based virtual screening; drug repurposing, docking; dynamics simulation.

1. INTRODUCTION

Zika virus (ZIKV) is a single stranded and positive sense RNA virus, Zika virus is a member of the family Flaviviridae along with other viruses like dengue virus and yellow fever virus [1,2]. Zika virus was isolated from a rhesus monkey in the Zika forest for the first time in Uganda in 1947 [3]. For a half century, sporadic cases of human infection with Zika virus were reported in both Africa and southeast Asia [4,5]. Then, in 2007 and 2013, two outbreaks of Zika virus were recognized in Yap island and French Polynesia respectively [6,7]. Later on, several outbreaks of ZIKV were recorded in Brazil between 2014 and 2016. These outbreaks of Zika virus were accompanied by a national increase of congenital neurological abnormalities [8]. As a result, the World Health Organization (WHO) have considered Zika virus infections and its possible neurological complications a worldwide public health emergency in 2016 [9]. Recent resurgence of *Aedes* mosquito, the known vector of Zika virus, in Mediterranean and Black sea regions can contribute significantly to future outbreaks of this virus in these areas [10].

Most cases of Zika virus infections are asymptomatic however some patients may be present with mild symptoms like fever, rash, fatigue and arthralgia. These mild symptoms can last for 2 to 7 days, and the incubation period of Zika virus infection can range between 3 and 12 days [3,11]. However, in utero infection with Zika virus during pregnancy can result in serious fetal neurological malformations like microcephaly [12]. Also, it is believed that infection with Zika virus can increase the incidence of Guillain-Barré syndrome. This syndrome is considered an autoimmune disease that influence peripheral nervous system leading to muscles weakness and possible paralysis [13]. As Zika virus can cause illness with nonspecific symptoms, diagnosis of ZIKV infection is still challenging. The most accurate diagnostic method depends on detection of Zika virus RNA in human body fluids by using reverse transcription polymerase chain reaction (RT-PCR). The application of serological tests like enzyme-linked immunosorbent assay (ELISA) is considered challenging due to ZIKV antibodies cross reactivity with those antibodies generated against other viruses of Flaviviridae family [14].

Zika virus is considered a mosquito borne disease, the virus can also be transmitted through blood transfusion and sexual contact. Vertical transmission of Zika virus is also possible where the mother can pass the virus to her fetus during pregnancy or to her newborn during delivery [15].

The RNA genome of Zika virus encodes a single polypeptide chain with a length of 3423 amino residues, this large polypeptide can be then cleaved by both host and viral protease enzymes into structural and non-structural proteins. Zika virus has three structural proteins and these are envelope (E), capsid (C) and pre-membrane (prM) proteins. These structural proteins are important for the creation of viral particles. Zika virus has also seven non-structural proteins including NS1, NS2A, NS2B, NS3, NS4A, NS4B, NS5. These non-structural proteins are essential for replication and assembly of viral particles. These proteins can also help the virus for evasion of immune system [1,16].

To date, neither vaccine nor drug has been developed against Zika virus. Different vaccine platforms like DNA plasmid and adenovirus based vector have been applied in animal models to induce protective immune response against Zika virus envelope (E) protein [3]. Regarding the development of anti-ZIKV drug, the NS2B/NS3 protease seems to be a potential molecular target to design and discover a candidate capable of inhibiting Zika virus ability to replicate inside host cells and escape immune defenses. This protease enzyme is composed of two main subunits, the first one is the non-structural protein NS3 with a protease activity at

its N-terminus and RNA helicase at its C-terminus. The second subunit is another non-structural protein, namely NS2B, that is membrane bound. NS2B subunit is considered important for proper orientation and functioning of Zika virus protease enzyme [16,17]. A three-dimensional view for Zika virus NS2B/NS3 protease can be seen in Fig. 1.

Structure based virtual screening is a computer-based approach capable of identifying hit candidates with potential activity against specific targets by using molecular docking and dynamics simulation [18]. Virtual screening approach can be applied to facilitate drug repurposing efforts. In drug repurposing, new uses are identified for an already approved drugs and beyond the original indications of these drugs. Thus, virtual drug repurposing can save both time and cost in drug development projects [19]. In this trend, two attempts for computer aided drug repurposing were able to recognize both the antihistamine chlorcyclizine and the antimalarial hydroxychloroquine as potential anti-ZIKV candidates. Both chlorcyclizine and hydroxychloroquine were predicted to have an inhibitory capacity against NS2B/NS3 protease according to virtual screening of approved drugs. Also, these two approved drugs appeared to be able to inhibit Zika virus viability in cell culture assay [17,20].

In this computational study, we have screened FDA approved drugs database against NS2B/NS3 protease crystal of Zika virus by using molecular docking and dynamics simulation. Our aim is to identify potential inhibitors of ZIKV protease enzyme through virtual drug repurposing.

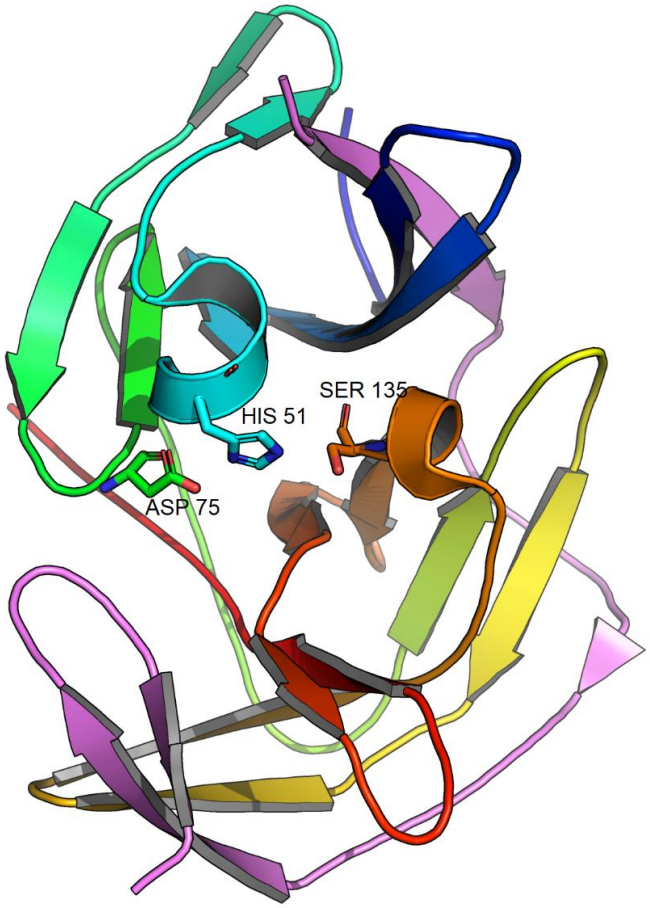

Fig. 1. A three-dimensional illustration for NS2B/NS3 protease crystal (PDB: 5H4I) of Zika virus. NS2B subunit is colored in violet while NS3 subunit is colored with rainbow gradient. The C-terminus of NS3 is shown in red and the N-terminus is colored by blue. Key residues of NS3 protease active site are represented as labeled sticks

2. METHODOLOGY

2.1 Setting up Virtual Screening Scheme

The project steps for virtual screening are outlined in Fig. 2. In summary, FDA approved drugs library were screened by docking software against Zika virus NS2B/NS3 protease crystal. Then the best 25 hits were selected and subjected to safety profile assessment by using online clinical reference. After that, only those safe hits were submitted to molecular dynamics (MD) simulation study. The ligands that can maintain both good binding energy and close proximity to protease crystal throughout simulation period were then selected for further elaboration.

2.2 Structure Based Virtual Screening

The steps of structure based virtual screening applied in this study is similar to those used in our previous projects [21–23]. Concisely, a library of FDA approved drugs was downloaded as SDF format from ZINC 15 database on June 01, 2021 [24]. This library contains 1615 chemical structures, and it was then uploaded to Mcule.com online discovery website for screening against NS2B/NS3 protease crystal of Zika virus [25]. The NS2B/NS3 protease crystal with code 5H4I was downloaded from Protein Data Bank as PDB format [26,27]. Upon uploading the target crystal to Mcule.com, the drug discovery platform automatically prepared the crystal for docking by using AutoDock tools [28]. Preparing the uploaded crystal by Mcule.com did include removing water molecules and any bound ligand from PDB file. It did also involve adding polar hydrogen and Gasteiger charges to the crystal. AutoDock Vina is embedded in Mcule.com to carry out structure based virtual screening [29]. For docking FDA approved drugs against protease crystal, we have used default parameters on Mcule.com website. The employed docking coordinates were (X: -8.5, Y: 4.0, Z: -17.0) and the area of binding site was (22 * 22 * 22) Angstrom. After docking, the hits were ranked according to their least binding energy to protease crystal. Finally, the top 25 drugs were selected for further consideration. Both PyMOL version 2.3 and Protein-Ligand Interaction Profiler (PLIP) web tool were used to visual three-dimensional and two-dimensional conformations for ligand-protease complex with least binding energy pose [30–32].

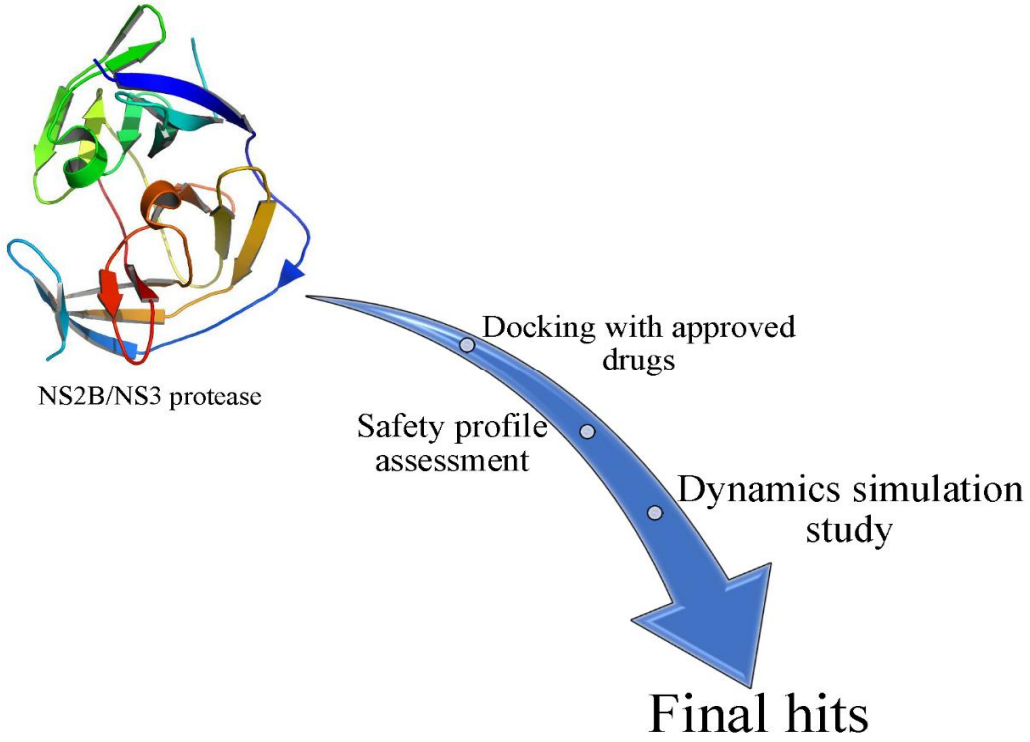

Fig. 2. Summary of virtual screening plan steps

2.3 Assessment of Safety Profile

We have used Medscape.com online clinical reference to evaluate the safety profile and the legal status for dispensing of the best 25 drugs of the virtual screening study [33]. Only those drugs with acceptable safety profile were then subjected to molecular dynamics (MD) simulation.

2.4 Molecular Dynamics (MD) Study

The top hits of the virtual screening study, with acceptable clinical safety profile, were then subjected to molecular dynamics (MD) analysis by using YASARA Dynamics version 20.12.24 [34]. The steps for MD study used here are similar to what we employed in our previous works [22,23,35]. For each hit, the ligand-protease complex with the least binding energy pose was submitted to MD simulation for 10 nanoseconds. The protocol of MD simulation did include optimization of hydrogen bonds and prediction of pKa to fine-tune protonation of amino acids at pH = 7.4 [36]. A 0.9% sodium chloride was used in MD simulation. To neutralize ligand-protease complex, an excess of sodium or chloride were added. To get rid of any clashes, both steepest descent and simulated annealing minimizations were utilized. The force fields applied during simulation were TIP3P for water, AMBER14 for solute, AM1BCC and GAFF2 for ligand [37–39]. Default parameters were used by AMBER, and the cutoff border for van der Waals forces was eight Angstrom [40]. For electrostatic forces, no cutoff limit was used due to the application of Particle Mesh Ewald algorithm [41]. Equations of motions were employed as multiple timestep of 1.25 femtoseconds and 2.5 femtoseconds for bonded and non-bonded interactions respectively at temperature of 298K and pressure of 1 atm [42]. After evaluation of solute Root Mean Square Deviation (RMSD) as a function of simulation time, the first 10 nanoseconds period was considered the equilibrium time and excluded from any further analysis. MD results for ligand movement RMSD and ligand conformation RMSD throughout simulation period were then plotted and visualized by using GraphPad Prism 8.0.2 [43].

The trajectories of MD simulation were then subjected for calculation of Molecular Mechanics Poisson-Boltzmann Surface Area (MM-PBSA) binding energy [44]. A built in YASARA macro was employed to facilitate estimation of MM-PBSA binding energy by using AMBER14 force field. According to YASARA guideline, the more positive binding energy indicates better interactions [45]. YASARA macro for binding energy calculation employs the following equation:

$$\text{Binding Energy} = \text{EpotRecept} + \text{EsolvRecept} + \text{EpotLigand} + \text{EsolvLigand} - \text{EpotComplex} - \text{EsolvComplex}$$

3. RESULTS AND DISCUSSION

For this structure based virtual screening study, the output hits were ordered according to their least energy of binding to Zika virus protease crystal. As seen in Table 1, we have selected only the top 25 hits and their docking energy was ranging between -8.5 and -7.3 Kcal/ mol. Based on this table, we can notice that all these hits are prescription only medications (POM) except the antidiarrheal agent Loperamide which is considered an over the counter (OTC) drug. According to a published cell culture-based project, low micromolar concentration of Loperamide was sufficient to inhibit the replicative capacity of Severe Acute Respiratory Syndrome Coronavirus (SARS-CoV), Middle East Respiratory Syndrome Coronavirus (MERS-CoV) and human coronavirus 229E [46]. Of interest, is the appearance of the antiretroviral drug Raltegravir and the penicillin antibiotic Nafcillin among these 25 hits. It is also worth mentioning that both Conivaptan and Azelastine were predicted to be potential inhibitors of SARS-CoV-2 main protease by our research group in a previous project [22]. Both Conivaptan and Azelastine were later proved to have activity against SARS-CoV-2 according to in vitro studies [47,48]. Additionally, Darifenacin is reported among the 25 hits in Table 1. The anti-muscarinic agent Darifenacin was previously predicted to have inhibitory capacity against several conserved molecular targets of SARS-CoV-2 by using both docking and dynamics simulation programs [49]. Then by reviewing the safety profile of these 25 drugs in Medscape clinical reference, only 14 hits were selected for further consideration and analysis. We have excluded 11 drugs that are approved by FDA for carcinoma, leukemia, schizophrenia, epilepsy and acne due to our concerns about the safety of these agents among general population.

Table 1. Chemical and clinical features of the top twenty-five hits that were docked against NS2B-NS3 protease of Zika virus; These drugs were ordered and ranked according to their least binding energy to the crystal of Zika virus NS2B-NS3 protease

No.	Generic name	Molecular formula	Energy of binding (Kcal/ mol)	Indication	Legal status
1	Conivaptan	$C_{32}H_{26}N_4O_2$	-8.5	Hyponatremia	POM
2	Olaparib	$C_{24}H_{23}FN_4O_3$	-8.2	Breast, ovarian and pancreatic cancers	POM
3	Adapalene	$C_{28}H_{28}O_3$	-8.1	Mild-moderate acne	POM
4	Paliperidone	$C_{23}H_{27}FN_4O_3$	-8.0	Schizophrenia	POM
5	Tolvaptan	$C_{26}H_{25}ClN_2O_3$	-7.9	Hyponatremia	POM
6	Difenoxin	$C_{28}H_{28}N_2O_2$	-7.9	Diarrhea	POM
7	Pimozide	$C_{28}H_{29}F_2N_3O$	-7.8	Schizophrenia	POM
8	Granisetron	$C_{18}H_{24}N_4O$	-7.8	Nausea and vomiting	POM
9	Raltegravir	$C_{20}H_{21}FN_6O_5$	-7.8	HIV	POM
10	Ezetimibe	$C_{24}H_{21}F_2NO_3$	-7.7	Hyperlipidemia	POM
11	Abemaciclib	$C_{27}H_{32}F_2N_8$	-7.7	Breast cancer	POM
12	Ponatinib	$C_{29}H_{27}F_3N_6O$	-7.7	Leukemia	POM
13	Ziprasidone	$C_{21}H_{21}ClN_4OS$	-7.7	Schizophrenia	POM
14	Indacaterol	$C_{24}H_{28}N_2O_3$	-7.6	Chronic obstructive pulmonary disease	POM
15	Pazopanib	$C_{21}H_{23}N_7O_2S$	-7.6	Soft tissue sarcoma and renal cell carcinoma	POM
16	Azelastine	$C_{22}H_{24}ClN_3O$	-7.6	Allergic rhinitis	POM
17	Alectinib	$C_{30}H_{34}N_4O_2$	-7.6	Non-small cell lung cancer	POM
18	Deferasirox	$C_{21}H_{15}N_3O_4$	-7.6	Iron overload	POM
19	Crizotinib	$C_{21}H_{22}Cl_2FN_5O$	-7.6	Non-small cell lung cancer	POM
20	Raloxifene	$C_{28}H_{27}NO_4S$	-7.6	Osteoporosis	POM
21	Darifenacin	$C_{28}H_{30}N_2O_2$	-7.4	Overactive bladder	POM
22	Perampanel	$C_{23}H_{15}N_3O$	-7.4	Epilepsy	POM
23	Chlortalidone	$C_{14}H_{11}ClN_2O_4S$	-7.4	Hypertension	POM
24	Nafcillin	$C_{21}H_{22}N_2O_5S$	-7.3	Gram-positive bacterial infection	POM
25	Loperamide	$C_{29}H_{33}ClN_2O_2$	-7.3	Diarrhea	OTC

POM: Prescription only medication; OTC: Over the counter

In the next step, only those 14 top hits with acceptable safety profile were then subjected to molecular dynamics (MD) simulation. MD study is considered an important tool in virtual screening field because it can predict ligand-target interactions by considering the flexibility of target [50]. For each hit, the ligand-protease complex with least binding energy pose was submitted to MD simulation for 10 nanoseconds. The summary of molecular dynamics study results can be seen in Table 2. In this table, we have reported the average binding energy by using Molecular Mechanics Poisson-Boltzmann Surface Area (MM-PBSA) calculation. According to YASARA Dynamics guideline, the more positive binding energy means better binding of the ligand. Also, we have presented in Table 2 the mean, minimum and maximum ligand movement Root-Mean-Square Deviation (RMSD) in Angstrom. The ligand movement RMSD was generated by superposing the receptor on its reference structure as a function of simulation period. Low ligand movement RMSD usually indicate close proximity to the target and hence better binding of the ligand. As such, potential inhibitor of NS2B/NS3 protease should have both low ligand movement RMSD and more positive MM-PBSA binding energy. By applying this condition to Table 2, only the anti-muscarinic agent Darifenacin and the anti-diarrheal agent Loperamide were selected as final hits for further evaluation.

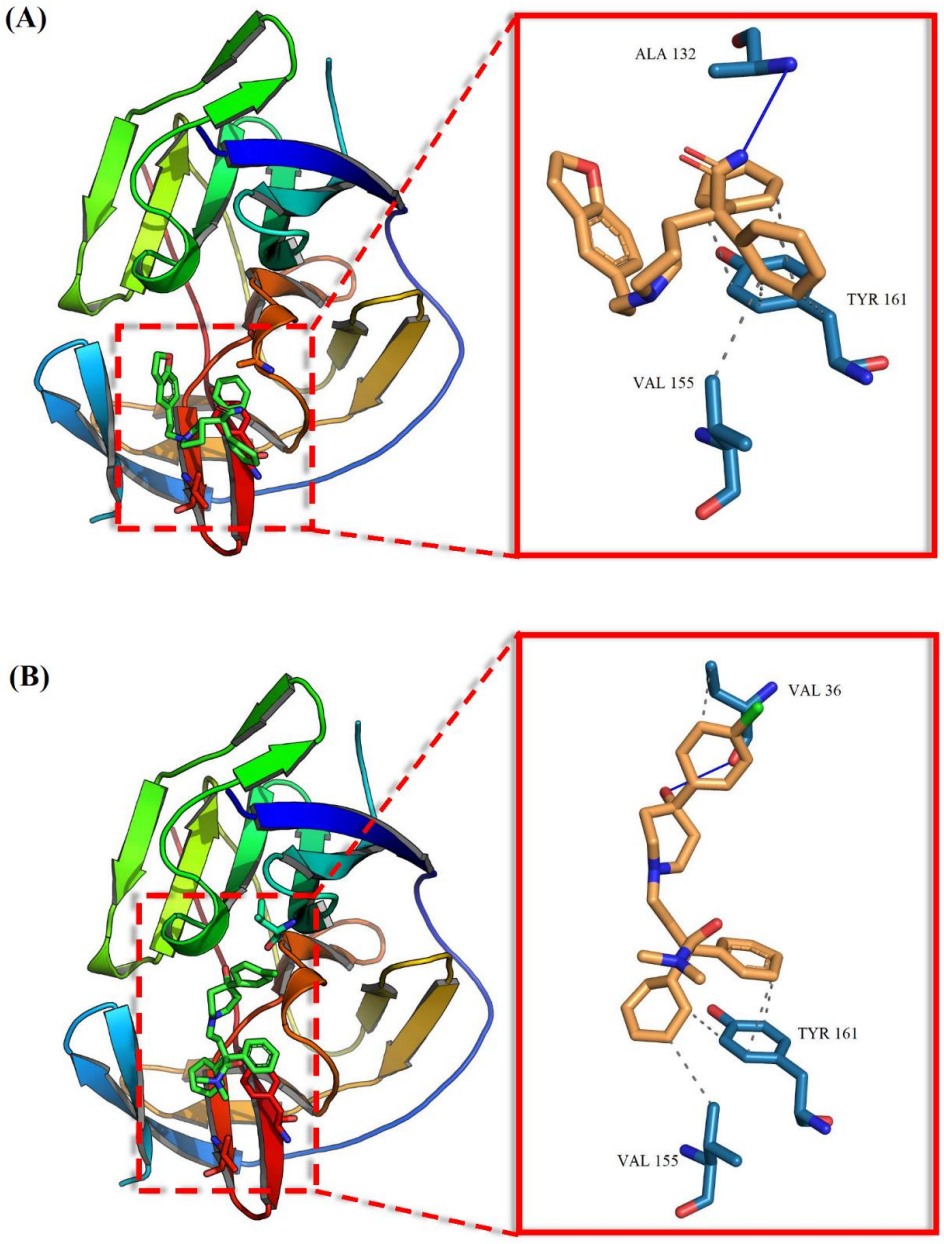

Fig. 3. Three-dimensional and two-dimensional views for the docking of (A) Darifenacin and (B) Loperamide against Zika virus NS2B/NS3 protease crystal. Hydrogen bond is presented as blue line while hydrophobic bond is displayed as dashed line

When examining docking images for Darifenacin and Loperamide in Fig. 3, we can notice that both drugs occupy almost same location within active site of NS2B/NS3 protease. According to Fig. 3, both Darifenacin and Loperamide are involved in hydrophobic interactions with valine 155 and tyrosine 161 residues of NS2B/NS3 protease complex. However, Darifenacin seems to be able to form hydrogen bonding with alanine 132. The alanine 132 is very close to serine 135 residue, the later residue is considered a key residue for the protease activity of NS2B/NS3 complex [17]. So, the ability of Darifenacin to form hydrogen bond with alanine 132 may influence access of substrate to serine 135 and adversely influence protease activity of NS2B/NS3 enzyme complex.

Table 2. Summary of dynamics simulation results for selected hits

No.	Drug name	Vina energy of binding (Kcal/ mol)	Average MM-PBSA binding energy (Kcal/ mol)	Ligand movement RMSD (Å)		
				Mean	Minimum	Maximum
1	Conivaptan	-8.5	-15.686	4.475	1.965	6.189
2	Tolvaptan	-7.9	-7.033	4.521	0.779	8.341
3	Difenoxin	-7.9	-17.075	2.683	0.765	5.476
4	Granisetron	-7.8	-27.128	3.283	1.655	4.826
5	Raltegravir	-7.8	-13.174	4.576	1.211	9.894
6	Ezetimibe	-7.7	-20.596	3.670	1.566	5.364
7	Indacaterol	-7.6	-41.571	2.692	1.047	3.103
8	Azelastine	-7.6	-28.072	2.725	1.288	4.209
9	Deferasirox	-7.6	-68.516	1.706	0.863	2.217
10	Raloxifene	-7.6	-97.377	5.621	1.668	7.029
11	Darifenacin	-7.4	-13.430	2.434	1.092	3.676
12	Chlortalidone	-7.4	-25.491	4.079	1.251	5.681
13	Nafcillin	-7.3	-6.360	4.663	1.29	6.544
14	Loperamide	-7.3	-34.862	1.965	1.086	2.683

MM-PBSA: Molecular Mechanics Poisson-Boltzmann Surface Area; RMSD: Root-Mean-Square Deviation; Å; Angstrom

Later on, we analyzed both ligand movement RMSD and ligand conformation RMSD throughout simulation time as seen in Fig. 4 and Fig. 5 respectively. As evident in Fig. 4, Loperamide can maintain a closer proximity throughout 10 nanoseconds than Darifenacin can do. In fact, it is obvious that Darifenacin movement RMSD has more fluctuations than that for Loperamide.

Regarding ligand conformation RMSD as a function of simulation duration, as seen in Fig. 5, it is clear that Darifenacin has undergo sharp fluctuation in conformation at the beginning of simulation and around 8 nanosecond point. This may explain the deviation experienced by Darifenacin in ligand movement RMSD in the same simulation points as can be noticed in Fig. 4. It is worth to clarify that ligand conformation RMSD was calculated by superposing the ligand on its reference structure throughout duration of simulation.

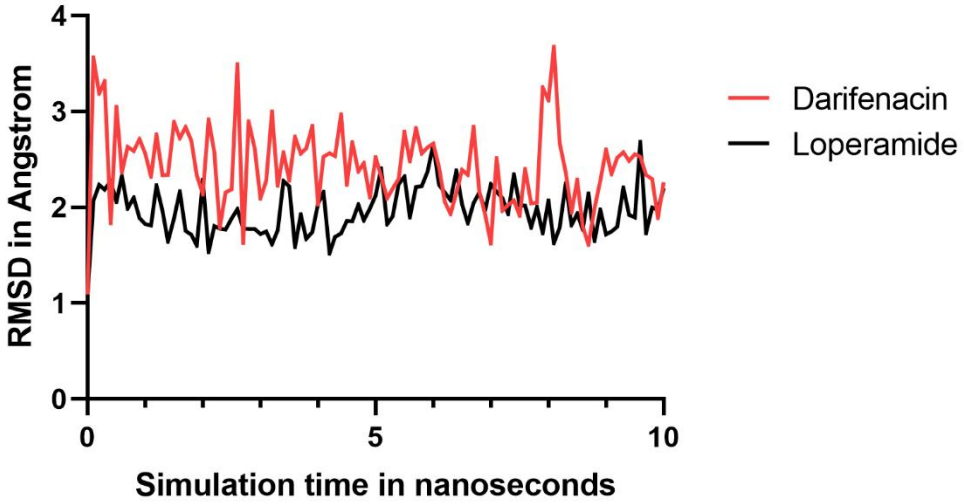

Fig. 4. Ligand movement RMSD as a function of MD simulation duration

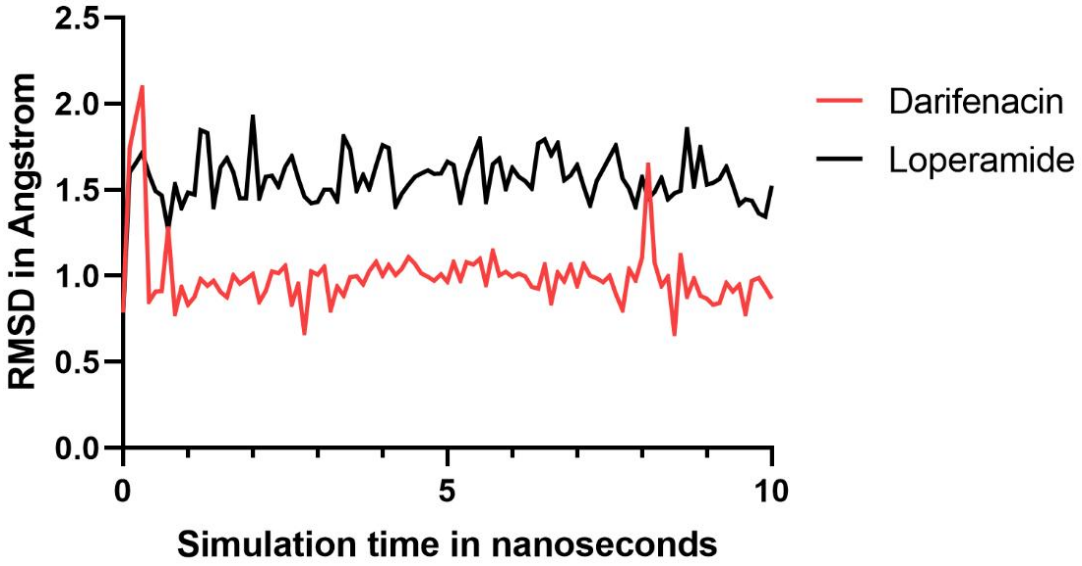

Fig. 5. Ligand conformation RMSD as a function of MD simulation time

4. CONCLUSION

In this study, we have applied structure based virtual screening approach to repurpose FDA approved drugs against Zika virus protease. Our project scheme did involve docking of 1615 approved drugs against NS2B/NS3 protease crystal, followed by evaluation of safety profile and dispensing regulations for the top 25 hits of docking output. Finally, only those top hits with acceptable safety records were subjected to molecular dynamics simulation. Here, we report that both antimuscarinic agent Darifenacin and antidiarrheal agent Loperamide may have potential capacity to inhibit NS2B/NS3 protease of Zika virus. Both drugs were able to maintain close proximity to protease active site throughout simulation. In addition, MM-PBSA calculation showed that both Darifenacin and Loperamide have favorable binding energy during simulation period. The antimuscarinic drug Darifenacin had more positive average MM-PBSA binding energy than did Loperamide. Also, Darifenacin was involved in hydrogen bonding with alanine 132 and this binding behavior may negatively impact substrate access to serine 135. The later residue is considered important for activity of protease enzyme. When compared to Darifenacin, Loperamide displayed a closer proximity to protease active site with lower tendency to fluctuate in terms of ligand movement RMSD and ligand conformation RMSD. However, these computational findings must be confirmed through invitro evaluation.

DISCLAIMER

The products used for this research are commonly and predominantly use products in our area of research and country. There is absolutely no conflict of interest between the authors and producers of the products because we do not intend to use these products as an avenue for any litigation but for the advancement of knowledge. Also, the research was not funded by the producing company rather it was funded by personal efforts of the authors.

COMPETING INTERESTS

Authors have declared that no competing interests exist.

REFERENCES

1. Kuno G, Chang GJJ. Full-length sequencing and genomic characterization of Bagaza, Kedougou, and Zika viruses. Arch Virol. 2007;152(4):687–96.
DOI: 10.1007/s00705-006-0903-z
2. Duong V, Dussart P, Buchy P. Zika virus in Asia. Int J Infect Dis. 2017;54:121–8.
DOI: 10.1016/j.ijid.2016.11.420
3. Poland GA, Kennedy RB, Ovsyannikova IG, Palacios R, Ho PL, Kalil J. Development of vaccines against Zika virus. Lancet Infect Dis. 2018;18(7):e211–9.
DOI: 10.1016/S1473-3099(18)30063-X

4. MacNamara FN. Zika virus: A report on three cases of human infection during an epidemic of jaundice in Nigeria. Trans R Soc Trop Med Hyg. 1954;48(2):139–45. DOI: 10.1016/0035-9203(54)90006-1
5. Olson JG, Ksiazek TG, Suhandiman G, Triwibowo V. Zika virus, a cause of fever in central java, indonesia. Trans R Soc Trop Med Hyg. 1981;75(3):389–93. DOI: 10.1016/0035-9203(81)90100-0
6. MR D, TH C, WT H, AM P, JL K, RS L, et al. Zika virus outbreak on Yap Island, Federated States of Micronesia. N Engl J Med. 2009;360(24):2536–43. DOI: 10.1056/NEJMOA0805715
7. D M, H B, HP M, M B, J B, L B, et al. Zika virus in French Polynesia 2013-14: anatomy of a completed outbreak. Lancet Infect Dis. 2018;18(5):e172–82. DOI: 10.1016/S1473-3099(17)30446-2
8. R L, C B, P B, OG C, NA H, H K, et al. The Zika Virus Epidemic in Brazil: From Discovery to Future Implications. Int J Environ Res Public Health. 2018;15(1). DOI: 10.3390/IJERPH15010096
9. A G. Zika virus is a global public health emergency, declares WHO. BMJ. 2016; 352:i657. DOI: 10.1136/BMJ.I657
10. Akiner MM, Demirci B, Babuadze G, Robert V, Schaffner F. Spread of the Invasive Mosquitoes Aedes aegypti and Aedes albopictus in the Black Sea Region Increases Risk of Chikungunya, Dengue, and Zika Outbreaks in Europe. PLoS Negl Trop Dis. 2016;10(4). DOI: 10.1371/JOURNAL.PNTD.0004664
11. W S, H S, AG A, AA M. Re-Emergence of Zika Virus: A Review on Pathogenesis, Clinical Manifestations, Diagnosis, Treatment, and Prevention. Am J Med. 2016;129(8):879.e7-879.e12. DOI: 10.1016/J.AMJMED.2016.02.027
12. MK W, HS W, J DB, KL T, K K. Zika virus: An emergent neuropathological agent. Ann Neurol. 2016;80(4):479–89. DOI: 10.1002/ANA.24748
13. VM C-L, A B, S M, S L, C R, J V, et al. Guillain-Barré Syndrome outbreak associated with Zika virus infection in French Polynesia: A case-control study. Lancet (London, England). 2016; 387(10027):1531–9. DOI: 10.1016/S0140-6736(16)00562-6
14. JJ W, BA P. Zika Virus: Diagnostics for an Emerging Pandemic Threat. J Clin Microbiol. 2016;54(4):860–7. DOI: 10.1128/JCM.00279-16
15. HM L, MS D. Zika Virus: New Clinical Syndromes and Its Emergence in the Western Hemisphere. J Virol. 2016;90(10):4864–75. DOI: 10.1128/JVI.00252-16
16. H C, FA A, MA H, A A, WH A, MA B, et al. Zika Virus Targeting by Screening Inhibitors against NS2B/NS3 Protease. Biomed Res Int. 2019;2019. DOI: 10.1155/2019/3947245
17. FRS S, DAF N, WG L, D D, LL S, AG T, et al. Identification of Zika Virus NS2B-NS3 Protease Inhibitors by Structure-Based Virtual Screening and Drug Repurposing Approaches. J Chem Inf Model. 2020; 60(2):731–7. DOI: 10.1021/ACS.JCIM.9B00933
18. AS R, H A, MJ M, R C-A, V A, T D. Recent applications of deep learning and machine intelligence on in silico drug discovery: methods, tools and databases. Brief Bioinform. 2019;20(5):1878–912. DOI: 10.1093/BIB/BBY061
19. S P, F I, PA E, KJ E, S H, A W, et al. Drug repurposing: Progress, challenges and recommendations. Nat Rev Drug Discov. 2019;18(1):41–58. DOI: 10.1038/NRD.2018.168
20. A K, B L, M A, SK S, N G, IU M, et al. Hydroxychloroquine Inhibits Zika Virus NS2B-NS3 Protease. ACS omega. 2018;3(12):18132–41. DOI: 10.1021/ACSOMEGA.8B01002
21. Odhar HA, Rayshan AM, Ahjel SW, Hashim AA, Albeer AAMA. Molecular docking enabled updated screening of the matrix protein VP40 from Ebola virus with millions of compounds in the MCULE database for potential inhibitors. Bioinformation. 2019;15(9):627–32. DOI: 10.6026/97320630015627
22. Odhar HA, Ahjel SW, Albeer AAMA, Hashim AF, Rayshan AM, Humadi SS. Molecular docking and dynamics simulation of FDA approved drugs with the main protease from 2019 novel coronavirus. Bioinformation. 2020;16(3): 236–44. DOI: 10.6026/97320630016236
23. Odhar HA, Ahjel SW, Hashim AF, Rayshan AM. Molecular Docking and Dynamics Simulation of a Screening Library from Life Chemicals Database for Potential Protein-Protein Interactions (PPIs) Inhibitors against SARS-CoV-2 Spike Protein. J Pharm Res Int. 2021;33:74–84.

DOI: 10.9734/JPRI/2021/V33I20A31350
24. Sterling T, Irwin JJ. ZINC 15 – Ligand Discovery for Everyone. J Chem Inf Model. 2015;55(11):2324–37.
DOI: 10.1021/ACS.JCIM.5B00559
25. Mcule. Accessed 2021 Jul 16.
Available:https://mcule.com/
26. RCSB PDB - 5H4I: Unlinked NS2B-NS3 Protease from Zika Virus in complex with a compound fragment.
Accessed 2021 Jul 16.
Available:https://www.rcsb.org/structure/5H4I
27. Z Z, Y L, YR L, WW P, AW H, C K, et al. Crystal structure of unlinked NS2B-NS3 protease from Zika virus. Science. 2016;354(6319):1597–600.
DOI: 10.1126/SCIENCE.AAI9309
28. Morris GM, Huey R, Lindstrom W, Sanner MF, Belew RK, Goodsell DS, et al. AutoDock4 and AutoDockTools4: Automated docking with selective receptor flexibility. J Comput Chem. 2009;30(16): 2785–91.
DOI: 10.1002/jcc.21256
29. Trott O, Olson AJ. AutoDock Vina: Improving the speed and accuracy of docking with a new scoring function, efficient optimization, and multithreading. J Comput Chem. 2009;31(2):NA-NA.
DOI: 10.1002/jcc.21334
30. PyMOL. Accessed 2021 Jul 16.
Available:https://pymol.org/2/
31. PLIP. Accessed 2021 Jul 16.
Available:https://plip-tool.biotec.tu-dresden.de/plip-web/plip/index
32. Adasme MF, Linnemann KL, Bolz SN, Kaiser F, Salentin S, Haupt VJ, et al. PLIP 2021: expanding the scope of the protein–ligand interaction profiler to DNA and RNA. Nucleic Acids Res. 2021;49(W1):W530–4.
DOI: 10.1093/NAR/GKAB294
33. Drug, OTCs & Herbals | Medscape Reference. Accessed 2021 Jul 16.
Available:https://reference.medscape.com/drugs
34. Krieger E, Vriend G. YASARA View - molecular graphics for all devices - from smartphones to workstations. Bioinformatics. 2014;30(20):2981–2.
DOI: 10.1093/bioinformatics/btu426
35. Odhar HA, Ahjel SW, Humadi SS. Towards the design of multiepitope-based peptide vaccine candidate against SARS-CoV-2. bioRxiv. 2020; 2020.07.07.186122.
DOI: 10.1101/2020.07.07.186122
36. Krieger E, Dunbrack RL, Hooft RWW, Krieger B. Assignment of protonation states in proteins and ligands: Combining pK a prediction with hydrogen bonding network optimization. Methods Mol Biol. 2012;819:405–21.
DOI: 10.1007/978-1-61779-465-0_25
37. Wang J, Wolf RM, Caldwell JW, Kollman PA, Case DA. Development and testing of a general Amber force field. J Comput Chem. 2004;25(9):1157–74.
DOI: 10.1002/jcc.20035
38. Maier JA, Martinez C, Kasavajhala K, Wickstrom L, Hauser KE, Simmerling C. ff14SB: Improving the Accuracy of Protein Side Chain and Backbone Parameters from ff99SB. J Chem Theory Comput. 2015;11(8):3696–713.
DOI: 10.1021/acs.jctc.5b00255
39. Jakalian A, Jack DB, Bayly CI. Fast, efficient generation of high-quality atomic charges. AM1-BCC model: II. Parameterization and validation. J Comput Chem. 2002;23(16):1623–41.
DOI: 10.1002/jcc.10128
40. Hornak V, Abel R, Okur A, Strockbine B, Roitberg A, Simmerling C. Comparison of multiple amber force fields and development of improved protein backbone parameters. Proteins Struct Funct Genet. 2006;65(3):712–25.
DOI: 10.1002/prot.21123
41. Essmann U, Perera L, Berkowitz ML, Darden T, Lee H, Pedersen LG. A smooth particle mesh Ewald method. J Chem Phys. 1995;103(19):8577–93.
DOI: 10.1063/1.470117
42. Krieger E, Vriend G. New ways to boost molecular dynamics simulations. J Comput Chem. 2015;36(13):996–1007.
DOI: 10.1002/jcc.23899
43. Prism - GraphPad. Accessed 2021 Jul 16.
Available:https://www.graphpad.com/scientific-software/prism/
44. JM S, RH H, JA M. Revisiting free energy calculations: A theoretical connection to MM/PBSA and direct calculation of the association free energy. Biophys J. 2004;86(1 Pt 1):67–74.
DOI: 10.1016/S0006-3495(04)74084-9
45. BindEnergyObj - Calculate binding energies. Accessed 2021 Jul 16.
Available:http://shaker.umh.es/yas/20.10.4/BindEnergyObj.html
46. De Wilde AH, Jochmans D, Posthuma CC, Zevenhoven-Dobbe JC, Van Nieuwkoop S, Bestebroer TM, et al. Screening of an

FDA-approved compound library identifies four small-molecule inhibitors of Middle East respiratory syndrome coronavirus replication in cell culture. Antimicrob Agents Chemother. 2014;58(8): 4875–84.
DOI: 10.1128/AAC.03011-14

47. Yang CW, Peng TT, Hsu HY, Lee YZ, Wu SH, Lin WH, et al. Repurposing old drugs as antiviral agents for coronaviruses. Biomed J. 2020;43(4):368–74.
DOI: 10.1016/J.BJ.2020.05.003

48. Ge S, Lu J, Hou Y, Lv Y, Wang C, He H. Azelastine inhibits viropexis of SARS-CoV-2 spike pseudovirus by binding to SARS-CoV-2 entry receptor ACE2. Virology. 2021;560:110–5.
DOI: 10.1016/J.VIROL.2021.05.009

49. Anand NM, Liya DH, Pradhan AK, Tayal N, Bansal A, Donakonda S, et al. A comprehensive SARS-CoV-2 genomic analysis identifies potential targets for drug repurposing. PLoS One. 2021;16(3):e0248553.
DOI: 10.1371/JOURNAL.PONE.0248553

50. Liu X, Shi D, Zhou S, Liu H, Liu H, Yao X. Molecular dynamics simulations and novel drug discovery. Expert Opin Drug Discov. 2018;13(1):23–37.
DOI: 10.1080/17460441.2018.1403419

Peer-review history:
The peer review history for this paper can be accessed here:
https://www.sdiarticle4.com/review-history/72038